Post-print of: Ordyszewska A., Szynkiewicz N., Perzanowski E., Chojnacki J., Wiśniewska A., Grubba R.: Structural and spectroscopic analysis of a new family of monomeric diphosphinoboranes. DALTON TRANSACTIONS. Vol. 48, iss. 33 (2019), pp. 12482-12495. DOI: 10.1039/C9DT02195G

Journal Name

ARTICLE

Received 00th January 20xx,

Accepted 00th January 20xx

DOI: 10.1039/x0xx00000x

www.rsc.org/

Structural and spectroscopic analysis of a new family of monomeric diphosphinoboranes

Anna Ordyszewska, Natalia Szynkiewicz, Emil Perzanowski, Jarosław Chojnacki, Aleksandra Wiśniewska, Rafał Grubba*

We present amino- and aryl- diphosphinoboranes $R_2PB(R'')PR'_2$ series, where R_2P, R'_2P = tBu$_2$P, tBuPhP, Ph$_2$P, Cy$_2$P, and R'' = iPr$_2$N, Ph, which were obtained *via* metathesis reaction of iPr$_2$NBBr$_2$ or PhBBr$_2$ with selected lithium phosphides. The structures of isolated diphosphinoboranes were characterized in the solid state and in the solution by means of X-ray diffraction and NMR spectroscopy, respectively. The utility of these P-B-P species as ligands for transition metal complexes was tested in reaction with [(COD)PtMe$_2$]. Moreover, we carried out DFT calculations to elucidate bonding interactions and philicity of the reactive centers as well as to analyze conformations of the studied species. Electronic and steric properties of substituents on P and B atoms were found to have a strong influence on the structures of obtained compounds. Three main types of diphosphanylboranes were distinguished, based on the strength of P-B π-interaction within the molecule: (i) application of strong electron-donating substituents on P-atoms and electron-accepting phenyl group on B atom led to the structure with one double P=B and one single P-B bond and diversified planar and pyramidal geometry of phosphanyl groups; (ii) reduction of the donor ability of phosphanyl groups gave diphosphanylboranes with delocalized P-B-P π-interactions; (iii) introduction of amino group with strong donor abilities on B atom canceled P-B π-interactions and allowed obtaining compounds with two very long P-B bonds and two pyramidal phosphanyl groups.

Introduction

Compounds containing linked boron and phosphorus atoms are receiving increasing interest due to their ambiphilic properties. These species have gained attention as a result of their potential applications as Frustrated Lewis Pairs (FLPs) in the activation of small molecules[1] and in coordination chemistry[2–6]. There are only two reviews on phosphinoboranes chemistry[2,7] which had been published within the 20-year time period and they are complementary to one another in time. First experiments concerning the synthesis of monomeric phosphinoboranes R_2PBR_2 resulted in head-to-tail polymerization yielding the $(R_2PBR_2)_n$ products[8]. It was stressed in the literature that the steric hindrance is crucial in order to obtain monomeric compounds since contrary dimeric $(R_2B\text{-}PR'_2)_2$, trimeric $(R_2BPR'_2)_3$ and cyclic compounds or even oligomers with four-coordinate phosphorus and boron atoms are formed[2,8–11]. It was not until 1961 when the first monomeric phosphinoborane Ph_2BPPh_2 was reported by Coates and Livingstone,[12] which was identified by quantitative oxidation reactions and characterized by IR spectroscopy. One year later the same researchers published a paper on the synthesis of aminophosphinoborane of the formula $(Me_2N)_2BPEt_2$ obtained as a result of the reaction between Et_2PLi and $(Me_2N)_2BCl$.[13] The chemistry of diphosphinoboranes was initiated by Coates and Livingstone also in 1961[14], when they synthesized the very first compound of this type $(Ph_2P)_2BPh$ in the reaction of diphenylphosphine Ph_2PH and dichlorophenylborane $PhBCl_2$ and the crystalline product was characterized using IR spectroscopy and cryoscopic molecular weight analysis[14]. The first amino(diphosphino)borane was synthesized not long after, when Nöth and Schrägle performed a reaction of Et_2PLi and Et_2NBCl_2 which resulted in the formation of $(Et_2P)_2BNEt_2$[13]. Another aminodiphosphinoborane $(Ph_2P)_2BNEt_2$ was obtained by Nöth and Sze in the elimination reaction of LiCl after mixing Ph_2PLi and Et_2NBCl_2[15]. Fritz and Hölderich used $(Me_3Si)_2PLi$ to perform a reaction with different aminoboranes R_2NBCl_2 (R=Me, Ph) yielding $R_2NB[P((Me_3Si)_2]_2$[16]. Only a few diphosphinoboranes were isolated in a crystalline form and therefore there are hardly any X-ray structures reported in the literature (Chart 1). The first well described is $(PPh_2)_2BMes$ which was synthesized by Power *et al.* in the reaction of Ph_2PLi with $MesBBr_2$.[17] The second $Ph_2NB[P(SiMe_3)_2]_2$ with crystallographic data was synthesized and characterized by Paine *et al*. along with many more examples of aminodiphosphinoboranes that have been described only by means of NMR spectroscopy.[18] Karsch *et al*. reported on the synthesis and isolation of $(Mes_2P)_2BX$ (X=Br, OEt). These diphosphinoboranes were obtained in the reaction of Mes_2PLi and BX_3 (X=Br, OEt).[19]

Department of Inorganic Chemistry, Faculty of Chemistry, Gdańsk University of Technology, G. Narutowicza St. 11/12. PL-80-233, Gdansk, Poland.

Electronic Supplementary Information (ESI) available: Experimental, crystallographic, spectroscopic and computational details. See DOI: 10.1039/x0xx00000x

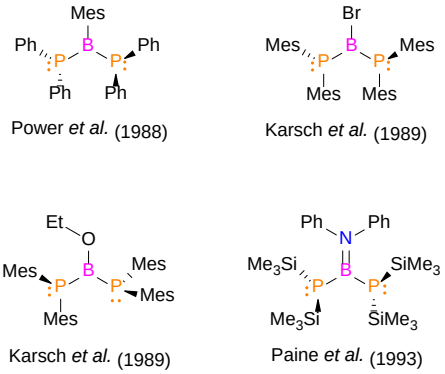

Chart 1. Schematic drawings of diphosphinoboranes with reported X-ray structures.

There are barely few papers containing transition metal complexes containing P-B-P ligands. The first isolated complex was described by Dou *et al*. who added $Cr(CO)_5 \cdot NMe_3$ to the solution of $iPr_2NB(PH_2)_2$ obtaining bimetallic compound $[iPr_2NB\{PH_2 \cdot Cr(CO)_5\}_2]$.[4] Peters et al. described the first Pt(II) and Ni(0) complexes having η^3-P,B,P coordinated ligands, which were obtained by the displacement of COD to give $[\{\eta^3\text{-}P,B,P\text{-}(PPh_2)_2BMes\}Pt(Me)_2]$ and $[\{\eta^3\text{-}P,B,P\text{-}(PPh_2)_2BMes\}Ni(COD)]$, respectively.[20] Helten, Pietschnig and co-workers described an iron complex with P-B-P bridge in the same year, where two different pathways lead to the formation of $Fe(C_5H_4PtBu)_2BMes$.[21]

Herein we present syntheses of the series of new, closely related diphosphinoboranes, together with a comprehensive analysis of their structural features. Moreover, we described the reactivity of these P-B-P ligands towards the platinum metal center.

Results and discussion

Syntheses of diphosphinoboranes

The main goal of this work was to determine the influence of substituents on the structure and reactivity of diphosphinoboranes. For this purpose, we have designed and synthesized a series of new, closely related compounds with a general formula $R_2PB(R'')PR_2'$(Chart 2). We have selected diversified R_2P phosphanyl building blocks which differ in electronic and steric properties. The nucleophilic properties and bulkiness of these groups decrease in the row: tBu_2P > Cy_2P > *t*BuPhP > Ph_2P. Furthermore, two different substituents were introduced on B atom: strongly electron-donating di*iso*propylamino group or electron-withdrawing - and less bulky phenyl substituent. It was essential for us to isolate related compounds in crystalline form and fully characterize their structures by means of X-ray diffraction. We anticipated that the mentioned substituents on B and P atoms should promote crystallization of the desired products.

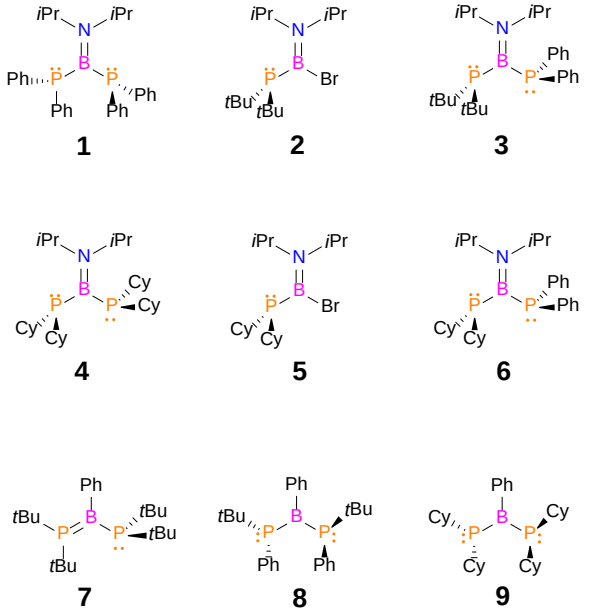

Chart 2. Diphosphinoboranes described in this work (including precursors **2** and **5**). The presented rotamers are in accord to XRD results.

In order to obtain diphosphinoboranes shown in Chart 2 we used a modified method of Power[17] and Paine[18] utilizing metathesis of phosphides and dihalogenoboranes. Synthetic procedure for obtaining amino(diphosphino)boranes **1** and **4** is presented in Scheme 1.

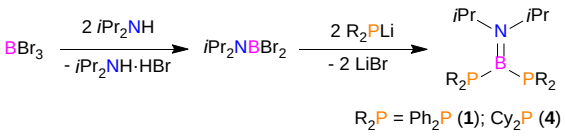

Scheme 1. Synthesis of amino(diphosphino)boranes.

The first step of this synthesis was a reaction of BBr_3 with two equivalents of di*iso*propylamine with the formation of amino(dibromo)borane and ammonium salt in petroleum ether at 0°C. Then the isolated borane iPr_2NBBr_2 reacted with two equivalents of R_2PLi, where R_2P = Ph_2P (**1**) or Cy_2P (**4**). The second step of the synthesis was performed in toluene where suspension of lithium phosphide was added to a solution of dibromoborane at -30 °C and then the mixture was allowed to warm up to room temperature yielding corresponding amino(diphosphino)boranes **1** and **4**. Monitoring the progress of reactions by ^{31}P and ^{11}B NMR spectroscopy revealed complete conversion of substrates after 2 days. The analysis of ^{31}P and ^{11}B NMR spectra indicated the formation of desired diphosphinoboranes **1** and **4** as main products (for NMR data of all isolated compounds see paragraph: *Multinuclear NMR spectroscopy)*. Additionally, weak signals of secondary phosphine R_2PH and traces of symmetrical diphosphanes $(R_2P)_2$ were present. These species are probably products of radical side-reactions and we observed them previously in every synthesis involving lithium phosphides.[22,23] X-ray quality crystals

of **1** and **4** were obtained from petroleum ether solutions at low-temperature in 81% and 16% yields, respectively.

A strong influence of the steric effect of phosphanyl group on the synthesis of diphosphinoboranes is manifested in the case of reaction involving tBu$_2$PLi. We did not observe a formation of postulated iPr$_2$NB(tBu$_2$)$_2$, even if a large excess of phosphide was added to amino(dibromo)borane. ^{31}P and ^{11}B spectroscopy indicated that this reaction stops at the stage of iPr$_2$NB(tBu$_2$)Br (**2**) and this product can be nicely obtained in the reaction of equimolar amounts of iPr$_2$NBBr$_2$ and tBu$_2$PLi (Scheme 2). It is worth stressing that analogous bromo-(phosphino)boranes possessing less crowded phosphanyl groups such as iPr$_2$NB(PCy$_2$)Br (**5**) can be also obtained using the same synthetic procedure (Scheme 2). Removing LiBr by filtration followed by evaporation of toluene from reaction solution gave analytically pure **2** as a white powder (yield 91%). The crystals suitable for X-ray analysis were formed by the slow evaporation of the solvent. Whereas the colorless crystals of **5** were obtained from a petroleum ether solution with a few drops of C_6D_6 at low temperature in 45% yield.

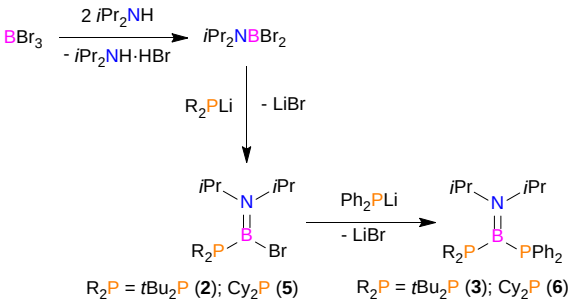

Scheme 2. Synthesis of amino(diphosphino)boranes with mixed phosphanyl substituents.

The successful isolation of **2** and **5** encouraged us to apply these species in the synthesis of diphosphinoboranes with mixed phosphanyl substituents. Indeed, we observed that **2** and **5** easily react with less bulky Ph$_2$PLi with the formation of corresponding diphosphinoboranes **3** and **6** (Scheme 2). The crystallization from petroleum ether solution at low temperature gave yellowish crystals **3** or **6** in 37 % and 50 % yield, respectively.

Subsequently, we carried out synthesis of series of B-aryl-substituted phosphinoboranes. In this two-step synthesis reaction of BBr$_3$ with PhSiMe$_3$ is followed by addition of two-fold excess of lithium phosphide to dibromo(phenyl)borane yielding diphosphinoboranes **7**, **8** or **9** (Scheme 3). We applied analogous reaction conditions as for the synthesis of amino(diphosphino)boranes described above.

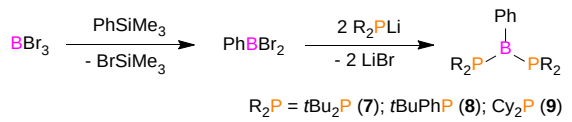

Scheme 3. Synthesis of aryl(diphosphino)boranes.

In contrast to experiments involving iPr$_2$NBBr$_2$, two voluminous tBu$_2$P groups can be introduced on boron atom, which was confirmed by isolation of **7** in good yield (59%) as big orange crystals. It is due to the smaller steric effect of phenyl group bonded to boron atom in comparison to the steric effect of di*iso*propylamino substituent. Two other aryl(diphosphino)boranes **8** and **9** were also isolated in crystalline form, however in significantly lower yields (14% and 3% respectively).

The compounds **1**-**9** are air sensitive and must be handled under inert atmosphere. They are very prone to hydrolysis which leads to R$_2$PH (**1**-**9**), iPr$_2$PH (**1**-**6**) and derivatives of boric acid (**1**-**9**).

Structural analysis

The simplest compounds containing trivalent, directly bonded phosphorus and boron atoms are phosphinoboranes. Their structures can be depicted by two extreme Lewis structures **a**-**b** shown in Chart 3. The phosphinoboranes of type **a** are isoelectronic with alkenes and their structural features are planar geometry at boron and phosphorus atoms and short P-B distance resulting from π-interaction of empty *p*-orbital of B atom with a lone pair at P atom. In contrast to **a**, structure **b** describes borylphosphine-like species with planar boryl group, pyramidal phosphanyl group and a long P-B bond. According to the classification proposed by Pringle[7] alkene-like compounds of type **a** have generally shorter P-B bonds than 1.88 Å and the sum of angles at P atoms greater than 330°.

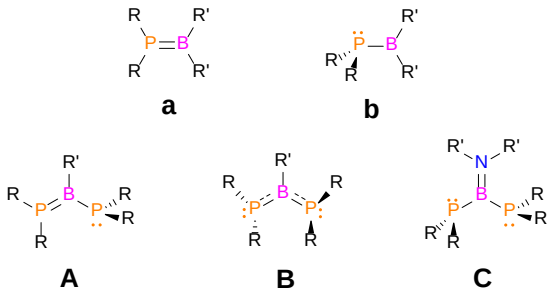

Chart 3. Comparison of structures of phosphinoboranes (**a**-**b**) and diphosphinoboranes (**A**-**C**).

A similar classification proposal can be created for diphosphinoboranes. Depending on their electronic structures we divided this class of compounds into three groups **A**, **B** and **C** depicted in Chart 3. In the case of structure **A** only one lone pair from one P-atom is involved in π-interactions with empty *p*-orbital of boron leading to one double and one single P-B bond. The structure **B** is isoelectronic with allyl anion where both lone pairs at P atoms are involved in P-B π-interactions, what is manifested by shortening of both P-B bonds and flattening of phosphanyl groups. The structure **C** describes species containing a strong electron donor group at boron atom, such as amino group, which decreases Lewis-acid abilities of B atom and cancels P-B π-bonding because of a better orbital size matching of B and N atoms in comparison to B and P atoms. The most characteristic features of the structure **C** are two pyramidal phosphanyl groups and two single P-B bonds.

The isolation of all obtained diphosphinoboranes in crystalline form allowed us to study their structural features in details based on the XRD results. Due to our knowledge, the full structural analysis was previously provided only for four monomeric diphosphinoboranes: $\{(Me_3Si)_2P\}_2BNPh_2$ (**I**);[18] $(Mes_2P)_2BOEt$ (**II**);[19] $(Mes_2P)_2BBr$ (**III**);[19] $(Ph_2P)_2BMes$ (**IV**).[17] The most significant metric parameters of diphosphinoboranes **1**, **3**-**4**, **6**-**9** and bromo(phosphino)boranes **2**, **5** along with the corresponding data of known diphosphinoboranes **I**-**IV** are collected in Table 1. Observably, amino(diphosphino)boranes **1**, **3**, **4** and **6** exhibit many similarities and therefore their structures are discussed together. Their molecular structures are shown in Figures 1, 2, S1 and S2, respectively. Common features of these compounds are planar geometry at B and N atoms, pyramidal geometry at P atoms, short B-N bond and very long P-B bonds. The B-N distances fall in the range of 1.392(3)-1.398(1) Å indicating double bond character of these bonds (sum of single bond covalent radii for B and N = 1.56 Å; sum of double bond covalent radii for B and N = 1.38 Å).[24,25] On the other hand, B-P distances are in the range of 1.972(3)-2.022(2) Å and they are even longer than typical distance for single covalent bond (sum of single bond covalent radii for B and P = 1.96 Å).[24]

Table 1. Selected bond lengths and geometries around B, P and N atoms for compounds **1**-**9**. Corresponding data for known diphosphinoboranes are also included: $\{(Me_3Si)_2P\}_2BNPh_2$ (**I**);[18] $(Mes_2P)_2BOEt$ (**II**);[19] $(Mes_2P)_2BBr$ (**III**);[19] $(Ph_2P)_2BMes$ (**IV**).[17]

No.	B1-P1 B1-P2 (Å)	B1-N1 (Å)	ΣB1 (°)	ΣN1 (°)	ΣP1 ΣP2 (°)
1	1.972(3) 1.976(4)	1.395(5)	359.8	360.0	318.0 314.9
2	1.958(2) -	1.389(2)	360.0	360.0	322.24 -
3	1.993(2)[a] 2.022(2)[a]	1.394(3)[a]	359.9[a]	359.95[a]	321.02[a] 315.26[a]
4	1.997(1) 1.995(2)	1.398(1)	359.99	359.8	320.61 303.05
5	1.958(2) -	1.387(2)	359.97	360.0	302.4 -
6	1.985(2) 2.004(2)	1.392(3)	360.0	359.9	303.6 312.65
7	1.964(1) 1.829(1)	-	359.15	-	321.36 355.43
8	1.876(1) 1.882(1)	-	360.0	-	327.58 325.33
9	1.874(2) 1.872(2)	-	360.0	-	331.08 331.37
I	1.895(7) 1.893(7)	1.465(8)	359.9	350.0	343.5 343.3
II	1.913(3) 1.951(3)	-	358.6	-	337.0 314.0
III	1.82(1) 1.84(1)	-	360.0	-	347.1 346.7
IV	1.901(2) 1.879(2)	-	360.0	-	318.8 324.5

[a] Average values for two molecules present in the independent part of the unit cell

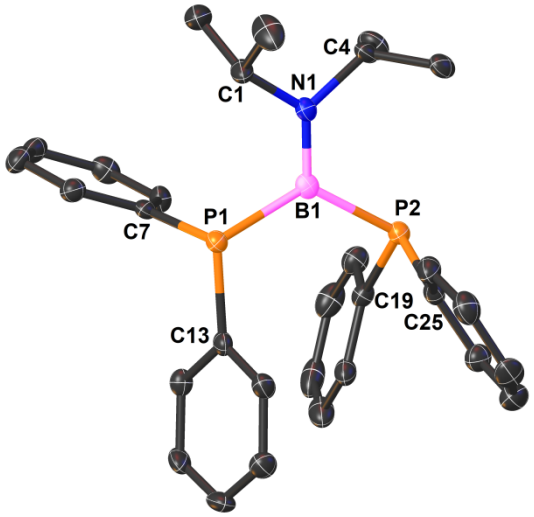

Figure **1**. X-ray structure of **1** showing the atom-numbering scheme. Ellipsoids are shown at 50% probability. H atoms have been omitted for clarity.

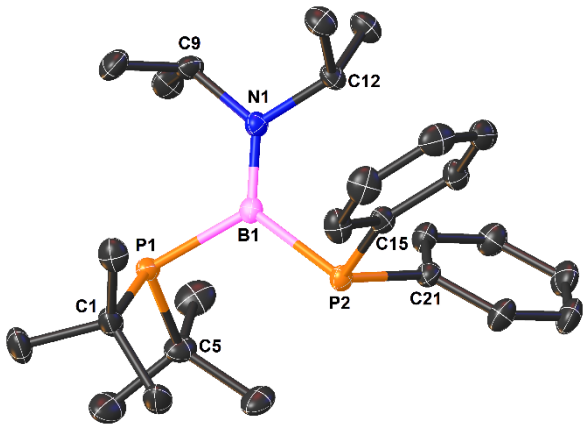

Figure **2**. X-ray structure of **3** showing the atom-numbering scheme. Ellipsoids are shown at 50% probability. H atoms have been omitted for clarity.

For **3** and **6** possessing mixed phosphanyl substituents on B atom, the B-P bonds are even longer than 2 Å what, on the basis of our best knowledge, makes them the longest distances reported for trivalent compounds of boron and phosphorus. **1** and **3**, **4**, **6** differ in the terms of conformation of phosphanyl groups. In the case of **1**, C13 atom of Ph_2P1 group is almost in an anti-coplanar position to B1-N1 bond (torsion C13-P1-B1-N1 = -177.35°), whereas the phenyl substituents of Ph_2P2 group exhibit anti-clinal conformation in respect of B1-N1 bond (torsion C19-P2-B1-N1 = -134.18°; C25-P2-B1-N1 = 113.11°). Diphosphinoboranes **3**, **4** and **6** display similar orientation of phosphanyl group where the first one is in anticlinal position to B1-N1 bond, whereas the second one possesses syn-clinal position with respect to this bond. It is observed that for **3** and **6** containing different R_2P groups, more bulky tBu$_2$P or Cy$_2$P moieties prefer anti-clinal orientation while less crowded Ph_2P shows syn-clinal position. Such molecular geometry minimizes the steric repulsion between the bulky phosphanyl groups such as tBu$_2$P or Cy$_2$P and NiPr$_2$ group. The comparison of known diphosphinoboranes structures **I**[18] and **II**[19] ,bearing donor NPh_2 or OEt groups at B atom respectively, with structures of **1**, **3**, **4**

and **6** reveals significant differences. In respect of amino(diphosphino)boranes described above **I** and **II** show shorter B-P bond distances and, in the case of **I,** weaker P-N π-interaction is manifested in longer B-N bond and less planar geometry at N atom (see Table 1). Structural differences between **I** and **1**, **3**, **4**, **6** can be explained by weaker donor abilities of Ph_2N group in comparison to iPr_2N substituent.

X-ray structures of bromo(phosphino)boranes **2** and **5** are shown in Figures 3 and S3, respectively. These compounds exhibit very similar structural features to **1**, **3**, **4** and **6** (Table 1). The geometries at B, N and P atoms in **2** and **5** resemble those in diphosphinoboranes described above. However, B-N and P-B bonds are slightly shorter than observed in **1**, **3**, **4** and **6**. Both compounds show anti position of *t*Bu or Cy substituents on P atom in respect of B1-N1 bond. Moreover, for both species, B-Br bond distances are very close to 1.99 Å which is a typical value for single covalent bond (sum of single bond covalent radii for B and Br = 1.99 Å).[24]

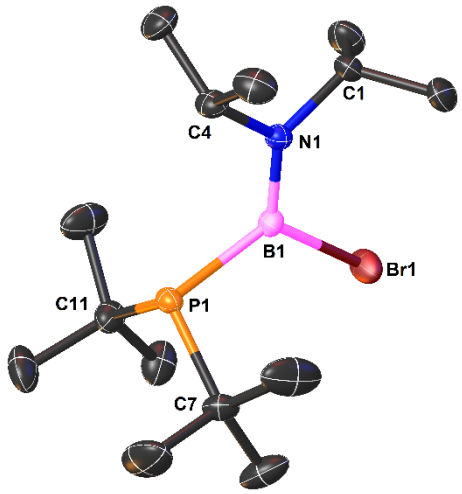

Figure **3**. X-ray structure of **2** showing the atom-numbering scheme. Ellipsoids are shown at 50% probability. H atoms have been omitted for clarity.

The electronic structures of **1**-**6** were studied by the natural bond orbitals (NBO) analysis. These results are fully consistent with X-ray structural data for **1**-**6**. Firstly, our calculations clearly indicate a double-bond character of the B–N bond within di- and phosphinoborane molecules resulting from strong interactions of lone pair at N and empty *p*-orbital at B atom. Secondly, B-P bonds in analyzed molecules are in fact single bonds. Moreover, the multiple B–N bond character and single B-P bond character were corroborated by the calculated Wiberg bond indexes, with values greater than 1 and close to 1, respectively (Table 2).

Table 2. Calculated Wiberg bond indexes (WBI) for selected bonds in **1**-**9**.

No.	B1-P1	B1-P2	B1-N1
1	1.0081	0.9623	1.1216
2	1.0201	-	1.1175
3	0.9798	0.9550	1.0744
4	0.9953	0.9643	1.0497
5	1.0077	-	1.1109
6	0.9746	0.9804	1.0875
7	1.0167	1.4449	-
8	1.2254	1.2254	-
9	1.2405	1.2289	-

Second order perturbation analysis allowed us to determine the importance of π-interactions between NBO orbitals of B and P atoms. The E(2) electron stabilization energy is associated with the electron density delocalization between the donor (lone pair at P-atom) and the acceptor (formally empty orbital at B-atom). The larger value of E(2), the stronger interaction between donor and acceptor and the greater extent of π-bonding. As it was expected, for the majority of amino-substituted species (**2**-**6**), due to the strong donor abilities of $NiPr_2$, interactions between lone pairs located at P-atoms and B-atom orbitals are negligible (E(2) < 0.5 kcal/mol). However, in the case of **1** such weak interactions are visible for P1 and B1 atom (E(2) = 9.11 kcal/mol). They can additionally stabilize the unusual conformation of **1**, where Ph group is in anti-coplanar position to B1-N1 bond. On the other hand, these weak interactions have no significant influence on B1-P1 bond length in **1**. The calculations of condensed Fukui functions provided information about the nucleophilicity and electrophilicity of the P,B,N-centers within molecules **1**-**6** (Table S13). These results indicate that **1**-**6** have dominantly nucleophilic character, where the strongest nucleophilic center is located on P-atom with values of f_N in the range of 0.313-0.169. The most nucleophilic character is attributed to P-atoms bearing *t*Bu or Cy groups while the introduction of Ph substituents reduces nucleophilic abilities of P centers. As it can be expected, electrophilic center in **1**-**6** is located on B-atom with values of f_E in the range of 0.116-0.159. Taking into account the results of X-ray diffraction and DFT-calculations, the structures of diphosphinoboranes **1**, **3**, **4** and **6** can be best depicted by Lewis structure **C** (Chart 3).
The introduction of phenyl substituent instead of an amino group at boron atom has a dramatic effect on the structure and bonding of diphosphinoboranes **7**, **8** and **9**. The molecular structure of $PhB(PtBu_2)_2$ (**7**) is shown in Figure 4 and its most important metric parameters are collected in Table 1. X-ray structure analysis revealed that the planar nature of B atom is also retained in **7**. However, both phosphorus centers exhibit diversified geometries, with pyramidal geometry at P1 atom (sum 321.36°) and almost planar geometry at P2 atom (sum 355.43°). Interestingly, P1, B1, C1, P2, lie almost in the same plane and C19 atom deviates from this plane only by 0.302 Å. The C15 atom of one remaining *t*Bu group at P2 atom deviates from P1B1C1P2 plane by -0.844 Å. The tBu_2P1 group exhibits syn-clinal orientation with respect to C1-B1 bond with torsions

C7-P1-B1-C1 = 38.77° and C11-P1-B1-C1 = -78.36°. Furthermore, in contrast to amino(diphosphino)boranes described above, both B-P bonds differ significantly in length with values 1.964(1) Å for B1-P1 and 1.829(1) Å for B1-P2. The short B1-P2 bond distance suggests a significant contribution of a multiple bonding (sum of single bond covalent radii for B and P = 1.96 Å; the sum of double bond covalent radii for B and P = 1.80 Å)[24,25] and falls in a typical range of B-P bond distances for phosphinoboranes with $R_2P{=}BR'_2$ structure.[7]

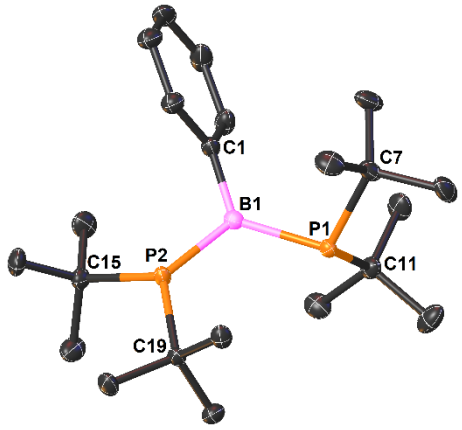

Figure **4**. X-ray structure of **7** showing the atom-numbering scheme. Ellipsoids are shown at 50% probability. H atoms have been omitted for clarity.

The almost planar geometry at P2 atom and short B1-P2 bond indicate an important interaction between *p*-orbital associated to lone pair at P2 atom with empty *p*-orbital of boron atom. Indeed, our DFT calculations fully support this interpretation. NBO analysis reveals sp^2 hybridization of P2 atom and dominated *p*-character of the lone pair at this atom. The orientation of $t\mathrm{Bu}_2$P2 phosphanyl group allows effective overlapping of unhybridized *p*-orbitals of P2 and B1 (Figure 5). Moreover, reduced occupancy of a donor *p*-orbital of P2 and increased occupancy of an acceptor *p*-orbital of B1 together with a relatively high value of stabilization energy E2, associated with delocalization of electron density between the donor (P2) and acceptor (B1), confirms the high contribution of π-bonding (Table 3). Furthermore, the values of Wiberg bond indexes for P1-B1 bond (1.02) and P2-B1 bond (1.44) differ significantly and point to a single bond character of the first one and multiple bond character of the second one. The structural and theoretical studies indicate that **7** is the first example of diphosphinoborane with one single and one double P-B bond and, due to the proposed classification of these species, it belongs to the type **A** (Chart 3).

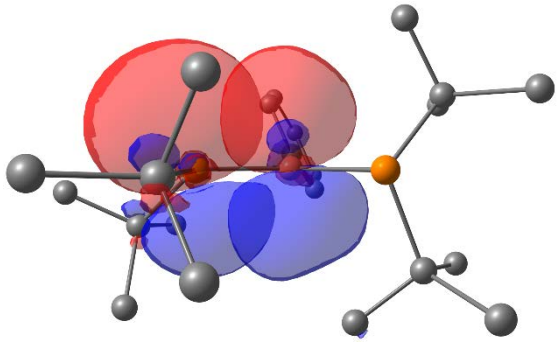

Figure **5**. Graphical representation of the NBOs of **7** involved in P-B π-interactions.

Table 3. Second order perturbation analysis of Fock matrix in NBO basis for selected donors and acceptors in **7**-**9**. E(2) is the stabilization energy associated with electron delocalization between donor and acceptor.

No.	donor	occupancy	acceptor	occupancy	E(2) (kcal/mol)
7	LP(P1) LP(P2)	1.90156 1.62911	LP*(B1)	0.41004	2.11 87.00
8	LP(P1) LP(P2)	1.78717 1.78717	LP*(B1)	0.39495	41.70 41.70
9	LP(P1) LP(P2)	1.77530 1.78213	LP*(B1)	0.42411	42.96 40.66

The molecular structures of **8** and **9** are presented in Figures 6 and S4, respectively. The structures of these diphosphinoboranes are very similar and will be discussed together. They differ in many aspects from amino(diphosphino)boranes **1**, **3**, **4**, **6** and aryl(diphosphino)borane **7** (Table 1).

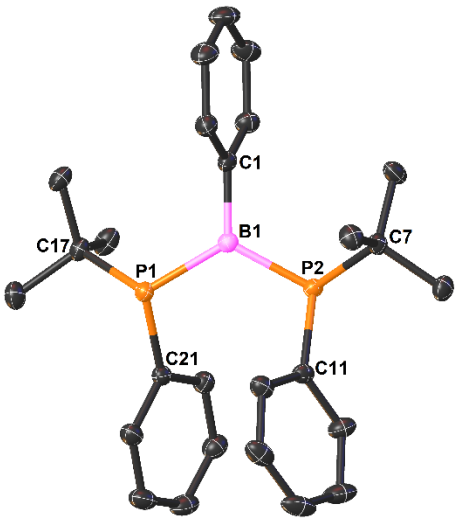

Figure **6**. X-ray structure of **8** showing the atom-numbering scheme. Ellipsoids are shown at 50% probability. H atoms have been omitted for clarity.

Similarly as in all studied diphosphinoboranes, boron atoms in **8** and **9** show planar geometry. In contrast to **7**, both P-atoms in **8** and **9** exhibit almost the same geometry and their coordinating polyhedrons are more planar in comparison to P atoms in amino(diphosphino)boranes **1**, **3**, **4**, **6** and P1 in **7**.

However, geometry at P1 and P2 is more pyramidal in comparison to P2 atom in **7**. Furthermore, in contrast to **7**, bond distances B1-P1/B1-P2 in **8** and **9** are almost equal with values 1.876(1)/1.882(1) for **8** and 1.874(2)/1.872(2) for **9**. These bond lengths are significantly shorter than analogous distances in amino(diphosphino)boranes and B1-P1 in **7**. However, they are noticeably longer than B1-P2 bond in **7**. The presence of two short and almost equal B-P bonds was also observed in previously reported $(Mes_2P)_2BBr$ (**III**)[19] and $(Ph_2P)_2BMes$ (**IV**)[17] (for comparison see Table 1). Diphosphinoboranes **8** and **9** differ from those described in this paragraph in terms of relative orientation of R substituents at P-atoms. In the case of **8** and **9**, two substituents (Ph in **8** or Cy in **9**) show anti-periplanar orientation to B1-C1 bond while two other R groups reveal syn-clinal position to this bond (*t*Bu in **8** or Cy in **9**). The substituents at P1 and P2 atoms point opposite directions in respect of P1B1P2C1 plane. The orientation of R_2P group in **8** and **9** resemble the one observed in previously reported **III**[19] and **IV**.[17] The structural features of **8** and **9** suggest a delocalization of π-interaction along P1-B1-P2 bonds. This finding is supported by NBO analysis conducted for these species. Our calculations revealed that in the case of **8** and **9**, both electron-donating P-centers contribute equally in π-interactions with electron-accepting B-center (Table 3). It is worth mentioning that relative orientation of phosphanyl groups allows effective overlapping of two orbitals associated with lone pairs at P-atoms with one formally empty *p*-orbital at B-atom (Figure 7).

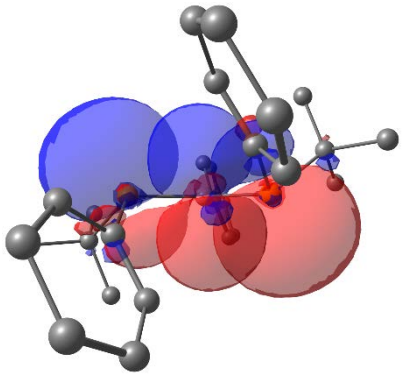

Figure **7**. Graphical representation of the NBOs of **8** involved in P-B-P π-interactions.

Furthermore, significant contribution of multiple bond character corroborates with Wiberg bond indexes for B1-P1 and B1-P2 bonds which have values greater than unity (Table 2). The analysis of condensed Fukui functions for **8** and **9** indicates ambiphilic character of these compounds (Table S13). Based on these findings, the electronic structure of **8** and **9** can be depicted by Lewis structure **B** (Chart 3).

Multinuclear NMR spectroscopy

The structures of **1**-**9** were investigated in the solution by ^{1}H, ^{11}B, $^{31}P\{^{1}H\}$ and $^{13}C\{^{1}H\}$ NMR spectroscopy. The $^{31}P\{^{1}H\}$ and ^{11}B chemical shifts for **1**-**9** are collected in Table 4.

Table 4. $^{31}P\{^{1}H\}$ and ^{11}B NMR data for compounds **1**-**9**.

No.	δ $^{31}P\{^{1}H\}$ (ppm)	δ ^{11}B (ppm)
1	-41.0	47.6
2	-11.2	38.6
3	-5.8 (tBu_2P), -40.5 (Ph_2P)	49.5
4	-43.3, - 44.1	52.4
5	-46.4	41.0
6	-39.3 (Ph_2P), -41.1 (Cy_2P)	50.2
7	54.7	68.6
8	42.7	80
9	28.0	71.1

The ^{11}B spectra of **1**-**9** exhibit broad resonances in a typical range for trivalent compounds of boron and phosphorous.[2] The observed signals of **1**-**9** in $^{31}P\{^{1}H\}$ spectra are also very broad. Because of this feature in $^{31}P\{^{1}H\}$ resonances, $^{1}J_{P\text{-}B}$ and $^{2}J_{P\text{-}P}$ couplings are not visible. Power proposed that for closely related species containing direct P-B bonds ^{31}P chemical shift provides useful information about the contribution of π-interactions within these bonds.[26] The larger positive values of chemical shift, the stronger interaction of lone pairs on P-atoms with electron-accepting B-center resulting in P-B π-delocalization. Indeed, this suggested correlation is clearly visible in the series **1**-**9**. The $^{31}P\{^{1}H\}$ resonances of **7**-**9** are strongly downfield shifted in comparison to respective resonances of amino-substituted species **1**-**6**. These spectroscopic results are in accord with structural and theoretical data for **7**-**9,** where significant multiple P-B bond character was observed. Broadening of signals in ^{11}B and $^{31}P\{^{1}H\}$ spectra of **1**-**9** can be explained not only by quadrupolar nature of boron but also by dynamic processes occurring in the solution at room temperature. Moreover, these processes are visible in ^{1}H spectra, where the resonances of the majority of studied compounds are also broad. Firstly, the rotation about the P-B bond is possible; secondly, the specific orientation of phosphanyl group can allow effective overlapping of *p*-orbitals of P and B atoms resulting in more planar geometry at P-atoms. Additionally, the structures in solution of **1**-**8** were investigated by recording VT-$^{31}P\{^{1}H\}$ and ^{1}H NMR spectra (see ESI for details). The dynamic behavior of **1**-**6** was studied by monitoring the splitting of the phosphanyl group signals in $^{31}P\{^{1}H\}$ spectra and splitting of the $CH(CH_3)_2$ and $CH(CH_3)_2$ signals of di*iso*propylamino group in ^{1}H spectra. Selected regions of VT-$^{31}P\{^{1}H\}$ and ^{1}H spectra of **1** are shown in Figure 8.

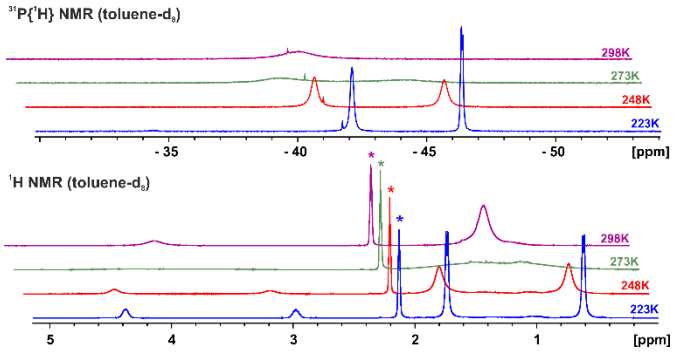

Figure **8**. Variable temperature $^{31}P\{^1H\}$ and ^1H spectra of **1** (*solvent residue signal).

The broad signal of R_2P group in the $^{31}P\{^1H\}$ spectrum of **1** at RT splits into two signals below 273 K. Similarly, below this temperature, in ^1H spectra of **1**, C**H**$(CH_3)_2$ and CH$(C\mathbf{H_3})_2$ signals split into two multiplets and into two doublets, respectively. These results point on free rotation about P-B bonds in **1** at room temperature. An analogous signal splitting was observed for **4** however it displays significantly higher coalescence temperature (318 K). In the case of diphosphinoboranes **3** and **6** the P-atoms and C**H**$(CH_3)_2$ and CH$(C\mathbf{H_3})_2$ protons are not equivalent both at room and lower temperatures and the number of signals does not change with the temperature however, the relevant signals become sharper at lower temperatures. Interestingly, in the case of $^{31}P\{^1H\}$ spectra of **3**, two strong singlets of tBu$_2$P and Ph$_2$P groups are accompanied by a pair of singlets with a much smaller intensity which can be attributed to the second conformer. Interesting information is provided by a comparison of VT-NMR spectra of amino(bromo)phosphinoboranes **2** and **5**. In VT-$^{31}P\{^1H\}$ spectra of **2** one singlet is observed, whereas in VT-^1H NMR spectra of this compound two signals of C**H**$(CH_3)_2$ protons and two signals attributed to CH$(C\mathbf{H_3})_2$ protons are present. In the case of **5** bearing less bulky Cy substituents, below 273 K corresponding signals are splitting into two singlets in $^{31}P\{^1H\}$ spectra and into four septets and four doublets in ^1H spectra, respectively. These observations indicate that two conformers are present in the solution of **5** at lower temperatures. The dynamic behavior in the solution is also observed for B-aryl-substituted phosphinoboranes **7** and **8** where it is manifested by the difference in the broadness of resonances in $^{31}P\{^1H\}$ and ^1H spectra with the change of temperature. To our surprise VT-$^{31}P\{^1H\}$ NMR spectra of **7** exhibit only one resonance, moreover VT-^1H NMR spectra of this compound contain only one multiplet (two broad lines with the same intensity and one broad line between with smaller intensity) attributed to tBu substituents on P-atoms. It is in contradiction with results of X-ray diffraction for **7** where a striking difference in geometry of P-centres was observed. These results show that **7** possess different conformations in a solution and solid state.

Notice, that the dynamic behavior of diphosphinoboranes in the solution can result from different processes: (i) rotation about the B-N bond, (ii) rotation about B-P bonds and (iii) rotation about N-C, P-C and B-C bonds. According to the literature data, rotational barrier about the B-N bond for monoaminoboranes has relatively high values ($\Delta G^{\ddagger}$ = 17-24 kcal/mol) and generally displays coalescence temperatures above 323 K.[27,28,29] The reported B-P rotation barriers $\Delta G^{\ddagger}$ for phosphinoboranes are in the range of 12-22 kcal/mol.[30] The N-C(iPr), P-C and B-C rotation barriers have values lower than 10 kcal/mol and exhibit coalescence temperature below 273K.[26,31,32,] As it was mentioned above $^{31}P\{^1H\}$ and ^1H NMR spectra of **1** and **4** display signals splitting at lower temperature. Hence, we were able to detect coalescence temperature and determine thermodynamic parameters $\Delta G^{\ddagger}$ and E_a of dynamic processes for **1** and **4** based on line-shape analysis of their VT-1H NMR spectra (see ESI for details). The temperatures of coalescence at 273K and 318K for **1** and **4** respectively suggested that observed dynamic process is related to the rotation about the B-P bonds. The obtained rotational barriers $\Delta G^{\ddagger}$ and E_a for **1** have values 12.8 kcal/mol and 10.3 kcal/mol respectively. As it was expected, corresponding barriers for **4** are higher ($\Delta G^{\ddagger}$ = 14.7 kcal/mol; E_a = 25.3 kcal/mol) due to the presence of more bulky Cy groups.

For further insight into structures of obtained compounds in the solution, we conducted conformational analysis by applying DFT calculations that were found to be in accord with VT-NMR experiments. The stereochemistry of diphosphinoboranes and bromo(phosphino)boranes was explored by the potential energy surfaces scaning (PESs) of the C-P-B-N (**1**-**6**) or C-P-B-C torsion angle (**7**-**8**) (Figure S91-S98, Tables S5-S12). Additionally, optimized structures of the most energetically privileged conformer (K1) together with the second low-energy conformer (K2) are presented for each compound in Figures S91-S98. For the majority of studied compounds (**1**-**5** and **8**) the predicted lowest energy conformation (conformer K1) corresponds to the form found in the crystal. The difference in the energies between highest-energy form and lowest-energy form (ΔE) increases proportionally with the bulkiness of the substituents on P and B atoms. For **1**, ΔE is found to be only 6.2 kcal/mol which is in accord with its dynamic behavior in the solution at room temperature. Introducing the voluminous tBu group at P atoms in amino-substituted species **2** dramatically increase ΔE value to 22.4 kcal/mol and inhibits rotation about the tBu$_2$P-B bond. The analogous situation is observed for (tBu$_2$P)(Ph$_2$P)BNiPr$_2$ (**3**) where rotation about the Ph$_2$P-B bond is clearly preferable. For species **4** and **5** containing Cy$_2$P groups, ΔE is even greater with values 28.6 kcal/mol and 26.1 kcal/mol, respectively. It is worth mentioning that ΔE values found for **1** and **4** correspond with the energy barriers derived from VT ^1H NMR experiments performed for these diphosphinoboranes (**1**: 6.2 vs 10.3 kcal/mol; **4**: 28.6 vs 25.3 kcal/mol). $^{31}P\{^1H\}$ and ^1H NMR spectra of **5** recorded below 273K revealed the presence of two conformers (K1, K1') in 1:1 molar ratio what implies the equal energy of these species. According to our calculations, these conformers possess the same C-P-B-N torsion angle and differ only in spatial orientation of iPr groups attached to N-atom (Figure S95), moreover they have almost the same energy (energy difference = 0.2 kcal/mol).

Predicted conformers K1 for **6** and **7** with the lowest energy differ from conformers found in the crystal - the X-ray structures of **6** and **7** are equivalent to the second predicted minimum K2.

The schematic drawings of the most energetically favored K1 forms for **6**-**7** are shown in Chart 3.

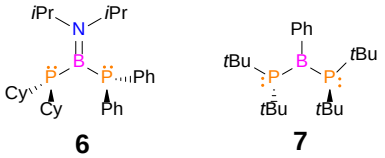

Chart 3. Schematic drawings of the calculated lowest-energy conformers (K1) for **6** and **7.**

Similarly to diphosphinoborane **3** with a mixed phosphanyl substituent, due to the difference in the steric effect of substituents at P-atoms, rotation about the B-PPh_2 bond in **6** is energetically more favored than rotation about the B-PCy_2 bond. In comparison to X-ray structure of **6**, the conformer K1 differs in position of C-atoms of Ph-groups bonded to the phosphorus atom, where the first one shows anti-periplanar position with respect to B-N bond whereas the second one exhibits anti-clinal orientation to this bond.

In contrast to amino-substituted compounds, **2** and **3** with the bulky *t*Bu_2P phosphanyl group, free rotation about the B-P*t*Bu_2 is possible for **7** at room temperature due to a less steric crowding at boron. Our calculations revealed a relatively small difference between the lowest- and the highest-energy conformers with ΔE value of 4.9 kcal/mol for this diphosphinoborane. As it was mentioned above, the lowest-energy conformer K1 of **7** shows a different structure from the one observed in the crystal (Chart 3, Figure S97). It exhibits fascinating structural features, where two tertiary C-atoms of two *t*Bu groups, two P-atoms, C-atom of Ph group bonded to boron and B-atom lie almost in the same plane. The tertiary C-atoms of two other *t*Bu groups point opposite directions in respect of this plane. NBO analysis of this conformer revealed that both *p*-orbitals attributed to the lone pairs at P-atoms interact equally with formally empty *p*-orbital at boron with very similar stabilization energies about 22.3 kcal/mol for both mentioned interactions (Figure 9).

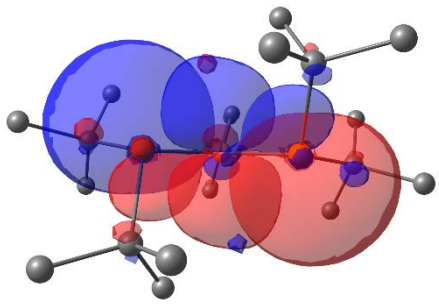

Figure 9. Graphical representation of the NBOs of **7** (the lowest-energy conformer K1) involved in P-B-P π-interactions.

Furthermore, both P-B distances are equal with values of 1.934 Å and both P-centers in this conformer show the same geometry with the sum of angles 326.67°. These results are in accord with VT-NMR studies of **7** where only one signal was observed for P-atoms in $^{31}P\{^1H\}$ spectrum and for *t*Bu group in ^1H spectrum. PES analysis of **8** reveals two minima, which differ in energy by ~7.0 kcal/mol, where the lowest-energy K1 conformer corresponds with X-ray structure. K2 differs from K1 in orientation of one phosphanyl *t*BuPhP group (anti position of *t*Bu and syn position of Ph in respect of B-C bond) (Figure S98).

Reactivity of diphosphinoboranes towards platinum metal center

Successful isolation of new diphosphinoboranes series allowed us to apply these compounds as polydentate ligands for transition metal centers. For this purpose we selected phosphinoboranes **1** and **7** which differ significantly in terms of bonding and steric crowding at boron and phosphorus atoms. The reaction of equimolar amounts of **1** and [(COD)$PtMe_2$] in toluene was monitored by $^{31}P\{^1H\}$ and ^{11}B NMR spectroscopy. The inspection of NMR spectra shows the quantitative formation of new complex **10** after 24 hours of stirring at room temperature (Scheme 4). The product starts to precipitate from toluene solution almost immediately.

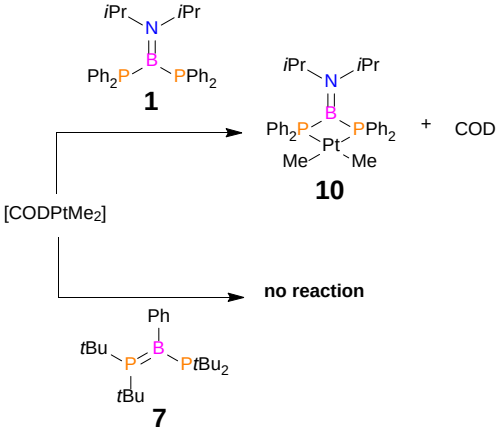

Scheme 4. Reactions of diphosphinoboranes **1** and **7** with [CODPtMe_2].

$^{31}P\{^1H\}$ NMR spectrum of **10** shows broad singlet at -24.6 ppm with platinum satellites ($^1J_{P\text{-}Pt}$ = 1406 Hz) which is upfield shifted in the comparison to **1** (Δδ = -16.4 ppm). Otherwise, the resonance in ^{11}B spectrum of **10** is almost unchanged in comparison to **1** (45.0 ppm (**10**) vs. 47.6 ppm (**1**)). These spectroscopic results clearly indicate complexation of **1** via both P-atoms without any significant interaction between Pt and B centers. The crystallization from CH_2Cl_2 gave yellow crystals of **10** in 38 % yield. In contrast to the reaction involving **1**, the diphosphinoborane **7** did not react with starting platinum complex, even after heating up (50°C) the reaction mixture for several days. This difference in reactivity of **1** and **7** can be explained by a greater steric effect of P*t*Bu_2 moiety in comparison to PPh_2 group. Due to our best knowledge, compound **10** is the first example of transition metal complex with amino(diphosphino)borane ligand. It is worth emphasizing that the transition metal complexes with diphosphinoborane ligands are very rare. Recently, the first examples of such complexes were reported, where Power's diphosphinoborane ($Ph_2P)_2$BMes (**IV**)[17] was used for the synthesis of [{η^3-*P,B,P*-($PPh_2)_2$BMes}Ni(COD)] and [{η^3-*P,B,P*-($PPh_2)_2$BMes}Pt($CH_3)_2$].[20] Unambiguous X-ray structure

determination of **10** allowed us to compare its structural feature with [{η³-*P*,*B*,*P*-$(PPh_2)_2$BMes}Pt$(CH_3)_2$].[20] The solid-state structure of **10** is shown in Figure 10.

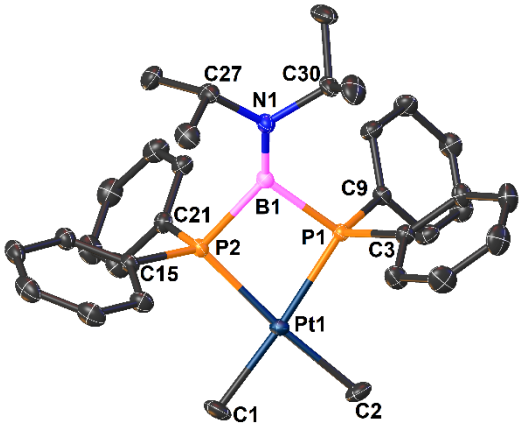

Figure **10**. X-ray structure of **10** showing the atom-numbering scheme. Ellipsoids are shown at 50% probability. H atoms have been omitted for clarity.

The X-ray structure analysis of **10** reveals tetra-coordinated platinum center which exhibits slightly distorted square planar geometry. The P1-B1 (1.984(3) Å), P2-B1 (1.978(3) Å) and B1-N1 (1.376(3) Å) are very similar to the corresponding distances in parent **1**. Furthermore, planar geometry at boron center (ΣB1 358.6°) and at nitrogen center (ΣN1 360.0°) is also retained. However, the Pt1-P1-B1-P2 ring is not planar but slightly folded along the P1-P2 vector. The Pt1-P1 (2.2866(7) Å), Pt1-P2 (2.2824(7) Å), Å Pt-C1 (2.088(3) Å) and Pt-C2 (2.081(4) Å) bond lengths are similar to those observed in [{η³-*P*,*B*,*P*-$(PPh_2)_2$BMes}Pt$(CH_3)_2$].[20] The very long Pt1-B1 distance 3.115(3) Å suggests an absence of bonding interaction between these atoms what was corroborated by ^{11}B NMR spectroscopy and our NBO calculations (Wiberg bond index for Pt1-B1 = 0.1). It is in contrast with the structure of platinum complex bearing aryl(diphosphino)borane ligand $(PPh)_2$BMes where short B-Pt distance was observed (2.403(11) Å).[20]

Conclusions

We have vastly expanded the family of monomeric diphosphinoboranes. We have shown that structures of these species can be easily designed by variation of substituents on boron or phosphorus atoms. This class of compounds is divided into three main groups which differ in terms of P-B-P π-bonding and geometry at P-atoms as was shown on Chart 3. They exhibit unprecedented structural features such as the longest P-B bonds observed for trivalent species of boron and phosphorus (**3**, **6**) or structure with one single and one double P-B bond (**7**). The presence of accessible lone pairs on both P-atoms makes amino(diphosphino)boranes useful bidentate ligands for transition metal complexation. Studies on application of these compounds in phosphinoboration of small inorganic and organic molecules are in progress and will be published due course.

Experimental part

Materials and methods

All experiments were carried out under argon atmosphere using Schlenk technique. All manipulations were performed using standard vacuum, Schlenk, and glove box techniques. All solvents were purified and dried using commonly known methods. Solvents for NMR spectroscopy (C_6D_6, toluene-d_8) were purified with metallic sodium/potassium. Phosphides[22], $PhSiMe_3$[33], $PhBBr_2$[34], *i*Pr_2NBBr_2, $CODPtCl_2$[35] and $CODPtMe_2$[36] were synthesized following the literature methods or using methods described below. BBr_3 and K_2PtCl_4 were purchased from commercial sources and used without further purification. *i*Pr_2NH was distilled prior to use. NMR spectra were recorded on a Bruker Avance III HD 400 MHz spectrometer at ambient or low temperature (external standard TMS for ^{1}H, ^{13}C; 85% H_3PO_4 for ^{31}P, $BF_3{\cdot}Et_2O$ for ^{11}B). The crystal structure analyses were performed on an STOE IPDS II diffractometer) using $Mo_{K\alpha}$ radiation (λ = 0.71073 Å). Elemental analysis was performed at the University of Gdańsk using a Vario El Cube CHNS apparatus.

Synthesis of *i*Pr_2NBBr_2

A solution of 20.2 g (200 mmol, 28 mL) of *i*Pr_2NH in 50 mL of petroleum ether was slowly added via the dropping funnel to an ice-cold solution of 26.4 g (100 mmol, 10 mL) BBr_3 in 400 mL of petroleum ether. The solution was allowed to warm up to room temperature and stirred overnight. The resulting precipitate of *i*$Pr_2NH{\cdot}HBr$ was removed by filtration and the solid residue was washed four times with 10 mL of petroleum ether. Then the solvent was evaporated from the filtrate and the residue was distilled under reduced pressure (10-12 mmHg, 67-70°C) yielding 11.0 g (41 mmol, yield 40%) of pure *i*Pr_2NBBr_2.

^{1}H NMR (C_6D_6, 400 MHz, δ): 3.73 (broad s, 2H, $(CH_3)_2C\mathbf{H}$), 0.98 (broad s, 12H, $(C\mathbf{H}_3)_2CH$)
^{11}B NMR (C_6D_6, 128 MHz, δ): 24.2 (s, N**B**Br_2)
$^{13}C\{^1H\}$ NMR (C_6D_6, 100 MHz, δ): 21.3 (broad s, $(\mathbf{C}H_3)_2CH$), 50.4 (very broad s, $(CH_3)_2\mathbf{C}H$)

General procedure for the syntheses of diphosphinoboranes

These syntheses are inspired by the previously described methods of Power[17] and Paine[18], where we used dibromoborane instead of dichloroborane to form amino(diphosphino)boranes. A suspension of R_2PLi (R= alkyl, aryl) in toluene was added dropwise to the solution of $R'BBr_2$ (R'= *i*Pr_2N, Ph) in toluene at -30 °C (although the addition can be done inversely by adding the solution of borane to phosphide as long as the same substituents on phosphorus atoms are considered). Then the reacting mixture was warmed up to room temperature and stirred overnight/for 2 days. The LiBr precipitate was further removed by filtration and the solvent was evaporated from the filtrate under reduced pressure. The residue was then dissolved in petroleum ether

(unless stated otherwise) in order to obtain the product in a crystalline form. Although the solid residue of the product is pure enough for further reactions after the evaporation of the solvent except for $(Cy_2P)_2BPh$ (**9**).

Synthesis of $(Ph_2P)_2BNiPr_2$ (1)

The suspension of 0.359 g (1.87 mmol) Ph_2PLi in 5 mL of toluene was added dropwise to the solution of 0.253 g (0.93 mmol) iPr_2NBBr_2 in 2.5 mL of toluene. The reacting mixture was stirred in a lower temperature for another 30 min and then warmed up to room temperature. Yellow crystals of **1** (0.364 g, 81% yield) were isolated at -30°C from the lemon-colored petroleum ether solution.

^{1}H NMR (tol-d_8, 400 MHz, 298 K, δ): 1.20 (s, broad, 12H, $(CH_3)_2CH$), 3.91 (s, very broad, 2H, $(CH_3)_2CH$), 6.95-7.51 (overlapped signals, 20 H, C_{Ar}-**H**)

^{1}H NMR (tol-d_8, 400 MHz, 223 K, δ): 0.62 (d, $^3J_{HH}$ = 6 Hz, 6H, $(CH_3)_2CH$), 1.73 (d, $^3J_{HH}$= 6 Hz, 6H, $(CH_3)_2CH$), 2.98 (m, $^3J_{HH}$≈ 6 Hz, 1H, $(CH_3)_2CH$), 4.38 (m, $^3J_{HH}$≈ 6 Hz, 1H, $(CH_3)_2CH$), 7.01 (m, overlapped, 10H, C_{Ar}-**H**), 7.10 (broad s, 2H, C_{Ar}-$\mathbf{H_p}$), 7.27 (broad t, $^3J_{HH}$= 7 Hz, 4H, C_{Ar}-$\mathbf{H_m}$), 7.80 (broad t, $^3J_{HH}$= 7 Hz, 4H, C_{Ar}-$\mathbf{H_o}$)

^{11}B NMR (C_6D_6, 128 MHz, 298 K, δ): 47.6 (broad s, (Ph_2P_2)**B**NiPr_2)

^{31}P{^{1}H} NMR (tol-d_8, 162 MHz, 298 K, δ): -40.7 (weak s, Ph_2PH), -41.0 (broad s, Ph_2**P**)

^{31}P{^{1}H} NMR (tol-d_8, 162 MHz, 223 K, δ): -41.7 (weak s, Ph_2PH), -42.1 (broad s, Ph_2**P**), -46.4 (broad d, $^3J_{PP}$= 9 Hz, Ph_2**P**)

^{13}C{^{1}H} NMR (C_6D_6, 100 MHz, 298 K, δ): 23.5 (broad s, $CH(CH_3)_2$), 52.9 (broad s, **C**H$(CH_3)_2$), 126.8 (s, $\mathbf{C_p}$), 127.9 (d, $^3J_{CP}$= 6 Hz, $\mathbf{C_m}$), 134.2 (d, $^2J_{CP}$= 18 Hz, $\mathbf{C_o}$), 137.7 (very broad d, $^1J_{CP}$≈ 14 Hz, $\mathbf{C_i}$);

Elemental analysis: calculated for $C_{30}H_{34}BNP_2$ (M= 481.36 g/mol): %C = 74.86 %, %H= 7.12 %, %N= 2.91 %, found: %C=74.54 %, %H= 7.13 %, %N= 2.74 %;

Synthesis of $(tBu_2P)(Br)BNiPr_2$ (2)

The suspension of 0.139 g (0.916 mmol) tBu_2PLi in 5 mL of toluene was added dropwise to the solution of 0.248 g (0.916 mmol) iPr_2NBBr_2 in 2.5 mL of toluene. The reacting mixture was stirred in a lower temperature for another 30 min and then warmed up to room temperature. A few crystals of **2** suitable for X-ray measurements were isolated after slow evaporation of the solvent. Analytically pure **2** was obtained by filtration of reaction mixture followed by the evaporation of the solvent (0.336 g, 91 % yield).

^{1}H NMR (C_6D_6, 400 MHz, 298 K δ): 0.94 (very broad s, 6H, $(CH_3)_2CH$), 1.39 (d, overlapped, $^3J_{PH}$= 12Hz, 18 H, $(CH_3)_3C$), 1.41, broad s, overlapped, 6H, $(CH_3)_2CH$), 3.22 (broad s, 1H, $(CH_3)_2CH$), 5.70 (broad s, 1H, $(CH_3)_2CH$)

^{1}H NMR (tol-d_8, 400 MHz, 223 K, δ): 0.87 (broad s, 6H, $(CH_3)_2CH$), 1.48 (broad s, overlapped, 18H, $(CH_3)_3C$), 1.48 (broad s, overlapped, 6H, $(CH_3)_2CH$), 3.24 (broad s, 1H, $(CH_3)_2CH$), 5.69 (broad s, 1H, $(CH_3)_2CH$)

^{11}B NMR (C_6D_6, 128 MHz, δ): 38.5 (broad s, $(tBu_2P)(Br)$**B**NiPr_2)

^{31}P{^{1}H} NMR (C_6D_6, 162 MHz, 298 K, δ): 19.6 (s, tBu_2**P**H), -11.2 (broad s, (tBu_2**P**))

^{31}P{^{1}H} NMR (tol-d_8, 162 MHz, 223K, δ): 17.0 (s, tBu_2**P**H), -14.8 (broad s, (tBu_2**P**))

^{13}C{^{1}H} NMR (C_6D_6, 100 MHz, δ): 20.6 (broad s, $(CH_3)_2CH$), 23.1 (broad s, $(CH_3)_2CH$), 31.7 (d, overlapped, $^2J_{CP}$≈ 21Hz, $(CH_3)_3C$), 31.8 (d, $^3J_{CP}$= 14Hz, $(CH_3)_3C$), 48.63 (very broad s, $(CH_3)_2CH$), 54.1 (very broad s, $(CH_3)_2CH$)

Elemental analysis: calculated for $C_{14}H_{32}BBrNP$ (M=336.10 g/mol): %C = 50.03%, %H= 9.60%, % N= 4.17%, found: %C= 49.98%, %H= 9.56%, % N= 4.09%;

Synthesis of $(tBu_2P)(Ph_2P)BNiPr_2$ (3)

The suspension of 0.151 g (0.786 mmol) Ph_2PLi in 5 mL of toluene was added dropwise to the solution of 0.226 g (0.786 mmol) $(tBu_2P)(Br)BNiPr_2$ in 2.5 mL of toluene. The reacting mixture was stirred in a lower temperature for another 30 min and then warmed up to room temperature. Analytically pure **3** was obtained by filtration of reaction mixture followed by the evaporation of the solvent (0.342 g, 97% yield). The crystallization in petroleum ether gave yellowish crystals of **3** (0.128 g, 37% yield).

^{1}H NMR (C_6D_6, 400 MHz, 298 K, δ): 0.60 (broad s, 6H, $(CH_3)_2CH$), 1.53 (d, $^3J_{HH}$= 11 Hz, 18H, $(CH_3)_3C$), 1.73 (broad s, 6H, $(CH_3)_2CH$), 3.19 (very broad s, 1H, $(CH_3)_2CH$), 4.50 (very broad s, 1H, $(CH_3)_2CH$), 7.01 (m, 2H, C_{Ar}-$\mathbf{H_p}$), 7.08 (m, 4H, C_{Ar}-$\mathbf{H_m}$), 7.54 (m, 4H, C_{Ar}-$\mathbf{H_o}$)

^{1}H NMR (tol-d_8, 400 MHz, 223 K, δ): 0.55 (d, $^3J_{HH}$= 7Hz, 6H, $(CH_3)_2CH$), 1.65 (d, $^3J_{HH}$= 12 Hz, 18H, $(CH_3)_3C$), 1.75 (d, $^3J_{HH}$= 6Hz, 6H, $(CH_3)_2CH$), 3.00 (m, $^3J_{HH}$= 7 Hz, 1H, $(CH_3)_2CH$), 4.47 (m, $^3J_{HH}$= 6 Hz, 1H, $(CH_3)_2CH$), 7.04 (m, 2H, C_{Ar}-$\mathbf{H_p}$), 7.12 (m, 4H, C_{Ar}-$\mathbf{H_m}$), 7.63 (t, $^3J_{HH}$= 7 Hz, 4H, C_{Ar}-$\mathbf{H_o}$)

^{11}B NMR (C_6D_6, 128 MHz, 298 K, δ): 49.5 (broad s, $(Ph_2P)(tBu_2P)$**B**NiPr_2)

^{31}P{^{1}H} NMR (C_6D_6, 162 MHz, 298 K, δ): -5.8 (broad s, tBu_2**P**), -40.5 (broad s, Ph_2**P**)

^{31}P{^{1}H} NMR (tol-d_8, 162 MHz, 223 K, δ): -10.7 (s, tBu_2**P**), -41.7 (s, Ph_2**P**)

^{13}C{^{1}H} NMR (C_6D_6, 100 MHz, 298 K, δ): 20.9 (broad s, $CH(CH_3)_2$), 26.9 (broad s, $CH(CH_3)_2$), 32.6 (broad d, $^2J_{CP}$= 24Hz, $C(CH_3)_3$), 33.2 (broad s, $C(CH_3)_3$)), 50.2 (broad s, **C**H$(CH_3)_2$), 56.9 (broad s, **C**H$(CH_3)_2$), 126.9 (s, $\mathbf{C_p}$), 128.2 (d, $^3J_{CP}$=6 Hz, $\mathbf{C_m}$), 134.3 (d, $^2J_{CP}$= 17 Hz, $\mathbf{C_o}$), 139.2 (very broad d, $^1J_{CP}$≈ 24 Hz, $\mathbf{C_i}$);

Elemental analysis: calculated for $C_{26}H_{42}BNP_2$ (M= 441.38 g/mol): %C = 70.75%, %H= 9.59%, %N= 3.17%, found: %C= 70.62%, %H= 9.53 %, %N= 3.17%;

Synthesis of $(Cy_2P)_2BNiPr_2$ (4)

The suspension of 0.415 g (2.03 mmol) Cy_2PLi in 5 mL of toluene was added dropwise to the solution of 0.275 g (1.016 mmol) iPr_2NBBr_2 in 2.5 mL of toluene. The reacting mixture was stirred in a lower temperature for another 30 min and then warmed up to room temperature. Colorless crystals of **5** (0.083 g, 16% yield) were isolated at -30°C from the yellowish petroleum ether solution. This compound exhibits low solubility in petroleum ether, however it is well soluble in toluene.

^{1}H NMR (tol-d_8, 400 MHz, 298K δ): 1.09 (very broad s, (CH_3)$_2$CH), 1.23-1.58 (m, overlapped, (CH_3)$_2$CH and CH_2 (Cy)), 1.73 (broad d, J≈ 12 Hz, CH_2 (Cy)), 1.82 (broad d, J≈ 12 Hz, CH_2 (Cy)), 2.02 (broad d, J≈ 12 Hz, CH_2 (Cy)), 2.42 (very broad s, CH (Cy)), 3.33 (broad s, (CH_3)$_2$CH), 4.41 (broad s, (CH_3)$_2$CH). Integration is not possible due to the overlapping of very broad signals.

^{1}H NMR (tol-d_8, 400 MHz, 223K, δ): 0.96 (d, $^3J_{HH}$ = 6Hz, 6H, (CH_3)$_2$CH), 1.44 (m, overlapped, 11H, CH_2 (Cy)), 1.60 (m, overlapped, 9H, CH_2 (Cy)), 1.74 (d, $^3J_{HH}$= 6Hz, 6H, (CH_3)$_2$CH), 1.81 (broad s, overlapped, 8H, CH_2 (Cy)), 1.92 (broad s, overlapped, 8H, CH_2 (Cy)), 2.12 (broad s, 4H, CH_2 (Cy)), 2.42 (broad m, 2H, CH (Cy)), 2.65 (broad s, 2H, CH (Cy)), 3.09 (broad m, $^3J_{HH}$≈ 6 Hz, 1H, (CH_3)$_2$CH), 4.31 (broad m, $^3J_{HH}$≈ 6 Hz, 1H, (CH_3)$_2$CH)

^{11}B NMR (C_6D_6, 128 MHz, δ): 52.4 (broad s, (Cy_2P)$_2$**B**N*i*Pr$_2$)

^{31}P{^{1}H} NMR (C_6D_6, 162 MHz, 298K, δ): -28.1 (s, Cy_2PH), -43.3 (broad s (Cy_2**P**)), -44.1 (broad s, (Cy_2**P**))

^{31}P{^{1}H} NMR (tol-d_8, 162 MHz, 223K, δ): -45.0 (broad s (Cy_2**P**)), -48.6 (s, (Cy_2**P**))

^{13}C{^{1}H} NMR (C_6D_6, 100 MHz, δ): 23.4 (s, (**C**H_3)$_2$CH), 26.6 (s, **C**H_2 (Cy)), 27.9 (broad m, **C**H_2 (Cy)), 34.0 (broad m, overlapped, **C**H_2 (Cy)), 34.6 (broad s, overlapped, **C**H (Cy)). Signals of (CH_3)$_2$**C**H are not visible.

Elemental analysis: calculated for $C_{30}H_{58}BNP_2$ (M= 505.55 g/mol): %C = 71.27 %, %H= 11.56 %, % N= 2.77 %, found: %C= 70.87 %, %H= 11.44 %, % N= 2.88%;

Synthesis of (Cy_2P)B(Br)N*i*Pr$_2$ (5)

The suspension of 0.207 g (1.016 mmol) Cy_2PLi in 5 mL of toluene was added dropwise to the solution of 0.275g (1.016 mmol) *i*Pr_2NBBr_2 in 2.5 mL of toluene. The reacting mixture was stirred in a lower temperature for another 30 min and then warmed up to room temperature. Colorless crystals of **5** (0.177 g, 45% yield) were isolated at -30°C from the colorless petroleum ether/C_6D_6 solution.

^{1}H NMR (tol-d_8, 400 MHz, 298 K δ): 1.00-1.41 (m, overlapped, 18H: 6H (**C**H_3)$_2$CH) and 12H C**H** (Cy)), 1.50 (broad m, 2H CH_2 (Cy)), 1.66 (d, $^3J_{HH}$= 12 Hz, 3H, (**C**H_3)$_2$CH), 1.74 (broad s, overlapped, 3H, (**C**H_3)$_2$CH), 1.75 (broad s, overlapped, 2H, CH_2 (Cy)), 1.90 (broad, s, 2H, C**H** (Cy)), 2.08 (broad s, 2H, C**H** (Cy)), 2.18 (broad m, 2H, CH_2 (Cy)), 3.37 (very broad s, (CH_3)$_2$C**H**), 5.31 (very broad s, (CH_3)$_2$C**H**) Due to the broadness of the signals, the integration of (CH_3)$_2$C**H**) is impossible.

^{1}H NMR (tol-d_8, 400 MHz, 223 K δ): 0.82 (d, $^3J_{HH}$= 6 Hz, 6H, (**C**H_3)$_2$CH) (**K1**), 0.93 (d, $^3J_{HH}$= 6 Hz, 6H, (**C**H_3)$_2$CH) (**K1'**), 1.30 (m, overlapped, 12H, C**H** (Cy)), 1.44 (broad d, 4H, C**H** (Cy)), 1.48 (d, $^3J_{HH}$= 7 Hz, 6H, (**C**H_3)$_2$CH) (**K1**), 1.59 (d, overlapped, $^3J_{HH}$= 7 Hz, 6H, (**C**H_3)$_2$CH) (**K1'**), 1.60 (broad s, overlapped 4H, C**H** (Cy)), 1.72 (broad d, 8H, C**H** (Cy)), 1.80 (broad s, 4H, C**H** (Cy)), 2.01 (broad s, 4H, C**H** (Cy)), 2.26 (broad s, 8H, C**H** (Cy)), 2.92 (m, $^3J_{HH}$= 7 Hz, 1H, (CH_3)$_2$C**H**) (**K1**), 3.02 (m, $^3J_{HH}$= 7 Hz, 1H, (CH_3)$_2$C**H**) (**K1'**), 5.15 (m, $^3J_{HH}$= 6 Hz, 1H, (CH_3)$_2$C**H**) (**K1**), 5.55 (m, $^3J_{HH}$= 6 Hz, 1H, (CH_3)$_2$C**H**) (**K1'**), where **K1** and **K1'** – two conformers present in the solution, although it is impossible to assign signals for Cy groups due to the overlapping.

^{11}B NMR(C_6D_6, 128 MHz, δ): 41.0 (broad s, (Cy_2P)**B**(Br)N*i*Pr$_2$)

^{31}P{^{1}H} NMR (C_6D_6, 162 MHz, 298K, δ): -28.0 (s, Cy_2PH), -46.4 (broad s, Cy_2**P**)

^{31}P{^{1}H} NMR (tol-d_8, 162 MHz,223, δ): -28.4 (s, Cy_2PH), -44.4 (broad s, Cy_2**P**), -47.2 (broad s, Cy_2**P**)

^{13}C{^{1}H} NMR (C_6D_6, 100 MHz, δ): 22.3 (very broad s, (**C**H_3)$_2$CH), 26.5 (s, **C**H_2 (Cy)), 27.2 (d, J_{CP}= 12 Hz, **C**H_2 (Cy)), 27.5 (d, J_{CP}= 8Hz, **C**H_2 (Cy)), 32.4 (d, J_{CP}= 11 Hz, **C**H_2 (Cy)), 33.3 (d, J_{CP}= 21 Hz, **C**H (Cy)), 35.4 (broad s, (**C**H_3)$_2$CH), 48.8 (very broad s, (CH_3)$_2$**C**H), 53.3 (very broad s, (CH_3)$_2$**C**H)

Elemental analysis: calculated for $C_{18}H_{36}BBrNP$ (M= 388.17 g/mol): %C= 55.69 %, %H= 9.35%, % N= 3.61 %, found: %C= 55.61 %, %H= 9.35 %, %N= 3.61%;

Synthesis of (Cy_2P)(Ph_2P)BN*i*Pr$_2$ (6)

The suspension of 0.204 g (1.06 mmol) Ph_2PLi in 5 mL of toluene was added dropwise to the solution of 0.287 g (1.06 mmol) $Cy_2PB(Br)NiPr_2$ in 5 mL of toluene. The reacting mixture was stirred in a lower temperature for another 30 min and then warmed up to room temperature. Yellowish crystals of **6** (0.183 g, 50 % yield) were isolated at -30°C from the pale yellow petroleum ether solution.

^{1}H NMR (tol-d_8, 400 MHz, 298 K δ): 0.79 (broad s, 6H, (**C**H_3)$_2$CH), 1.23 (broad s, overlapped, 6H, C**H** (Cy)), 1.41 (broad d, 4H, C**H** (Cy)), 1.65 (broad s, 4H, C**H** (Cy)), 1.72 (s, overlapped, 2H, C**H** (Cy)), 1.72 (broad s, overlapped, 6H, (**C**H_3)$_2$CH), 1.98 (broad d, 4H, C**H** (Cy)), 2.17 (broad s, 2H, C**H** (Cy)), 3.28 (very broad s, 1H (CH_3)$_2$C**H**), 4.49 (very broad s, 1H (CH_3)$_2$C**H**), 7.06 (broad s, 1H, C_{Ar}-**H$_p$**), 7.08 (broad s, 1H, C_{Ar}-**H$_p$**) 7.12 (d, overlapped, 1H, C_{Ar}-**H$_o$**), 7.13 (s, overlapped, 2H, C_{Ar}-**H$_o$**), 7.15 (m, 1H, C_{Ar}-**H$_o$**), 7.58 (t, $^3J_{HH}$= 7 Hz, 4H, C_{Ar}-**H$_m$**)

^{1}H NMR (tol-d_8, 400 MHz, 223 K, δ): 0.75 (d, $^3J_{HH}$= 6Hz, 6H, (**C**H_3)$_2$CH), 1.21 (very broad d, 2H, C**H** (Cy)), 1.28 (very broad d, 4H, C**H** (Cy)), 1.47 (very broad d, 2H, C**H** (Cy)), 1.59 (very broad d, 2H, C**H** (Cy)), 1.72 (broad s, 4H, C**H** (Cy)), 1.79 (d, $^3J_{HH}$ = 6Hz, 6H, (**C**H_3)$_2$CH), 1.85 (broad s, 2H, C**H** (Cy)), 2.00 (broad d, 2H, C**H** (Cy)), 2.19 (very broad s, 4H, C**H** (Cy)), 3.08 (m, $^3J_{HH}$= 6 Hz, 1H, (CH_3)$_2$C**H**), 4.53 (m, $^3J_{HH}$= 6 Hz, 1H, (CH_3)$_2$C**H**), 7.08 (d, $^3J_{HH}$= 7 Hz, 2H, C_{Ar}-**H$_p$**), 7.13 (overlapped, 3H, C_{Ar}-**H$_o$**), 7.20 (s, 1H, C_{Ar}-**H$_o$**), 7.66 (t, $^3J_{HH}$= 7 Hz, 4H, C_{Ar}-**H$_m$**)

^{11}B NMR (C_6D_6, 128 MHz, δ): 50.2 (broad s, (Cy_2P)(Ph_2P)**B**N*i*Pr$_2$)

^{31}P{^{1}H} NMR (C_6D_6, 162 MHz, 298K, δ): -14.9 (s, Ph_2P–PPh_2), -39.3 (broad s,Ph_2**P**), -41.1 (broad s, Cy_2**P**)

^{31}P{^{1}H} NMR (tol-d_8, 162 MHz, 223K, δ): -16.0 (s, Ph_2P–PPh_2), -40.2 (broad s,Ph_2**P**), -43.0 (broad s, Cy_2**P**)

^{13}C{^{1}H} NMR (C_6D_6, 100 MHz, δ): 21.0 (broad s, (**C**H_3)$_2$CH), 26.5 (s, overlapped, **C**H, (Cy)), 26.8 (very broad s, (**C**H_3)$_2$CH), 27.4 (d, overlapped, J_{CP}= 10 Hz, **C**H (Cy)), 33.5 (t, J= 11Hz, **C**H, (Cy)), 34.3 (d, overlapped, J_{CP}= 15 Hz, **C**H (Cy)), 49.6 (broad s, (CH_3)$_2$**C**H), 56.3 (broad s, (CH_3)$_2$**C**H), 127.2 (s, overlapped, **C$_p$**), 128.2 (d, overlapped, $^2J_{CP}$= 7 Hz, **C$_o$**), 134.9 (d, $^3J_{CP}$= 18 Hz, **C$_m$**), 139.0 (d, $^1J_{CP}$=14 Hz **C$_i$**)

Elemental analysis: calculated for $C_{30}H_{46}BNP_2$ (M= 493.45 g/mol): %C= 73.02 %, %H= 9.40 %, N= 2.84 %, found: %C= 73.06 %, %H= 9.38 %, % N= 2.74 %;

Synthesis of (*t*Bu$_2$P)$_2$BPh (7)

The suspension of 0.491 g (3.22 mmol) *t*Bu$_2$PLi in 5 mL of toluene was added dropwise to the solution of 0.400 g (1.61 mmol) PhBBr$_2$ in 2.5 mL of toluene. The reacting mixture was stirred in a lower temperature for another 30 min and then warmed up to room temperature. Big orange crystals of **7** (0.357 g, 59% yield) were isolated at - 30°C from the orange-colored petroleum ether solution.

^{1}H NMR (C_6D_6, 400 MHz, 298K, δ): 1.47 (m, overlapped, 36H, (C**H**$_3$)$_3$C), 7.09 (t, $^3J_{HH}$= 7 Hz, 1H, C$_{Ar}$-**H$_p$**), 7.17 (t, $^3J_{HH}$= 7 Hz, 2H, C$_{Ar}$-**H$_m$**), 7.54 (d, $^3J_{HH}$= 7 Hz, 2H, C$_{Ar}$-**H$_o$**)
^{1}H NMR (tol-d$_8$, 400 MHz, 223 K, δ): 1.47 (m, overlapped, 36H, (C**H**$_3$)$_3$C), 7.13 (m, $^3J_{HH}$≈ 7 Hz, 1H, C$_{Ar}$-**H$_p$**), 7.22 (m, $^3J_{HH}$≈ 7 Hz, 2H, C$_{Ar}$-**H$_m$**), 7.60 (d, $^3J_{HH}$= 7 Hz, 2H, C$_{Ar}$-**H$_o$**)
^{11}B NMR(C_6D_6, 128 MHz, δ): 68.6 (broad s, (*t*Bu$_2$P)$_2$**B**Ph)
^{31}P{^{1}H} NMR (tol-d$_8$, 162 MHz, 298 K, δ): 19.7 (s, *t*Bu$_2$**P**H), 54.7 (broad s, *t*Bu$_2$**P**)
^{31}P{^{1}H} NMR (tol-d$_8$, 162 MHz, 223K, δ): 16.9 (s, *t*Bu$_2$**P**H), 50.1 (broad s, *t*Bu$_2$**P**)
^{13}C{^{1}H} NMR (C_6D_6, 100 MHz, δ): 34.03 (d, overlapped, $^3J_{CP}$≈ 6 Hz, C(**C**H$_3$)$_3$), 36.77 (s, **C**(CH$_3$)$_3$), 126.67 (s, **C$_p$**), 126.81 (s, **C$_m$**), 132.1 (t, $^3J_{CP}$ = 9Hz, **C$_o$**), 147.0 (**C$_i$** – on the basis of HMBC spectrum)
Elemental analysis: calculated for $C_{22}H_{41}BP_2$ (M= 378.32 g/mol): %C = 69.84 %, %H= 10.92 %, found: %C= 69.40 %, %H= 10.73 %;

Synthesis of (*t*BuPhP)$_2$BPh (8)

The suspension of 0.331 g (1.92 mmol) *t*BuPhPLi in 7 mL of toluene was added dropwise to the solution of 0.238 g (0.96 mmol) PhBBr$_2$ in 2.5 mL of toluene. The reacting mixture was stirred in a lower temperature for another 30 min and then warmed up to room temperature. Analytically pure **8** was obtained by filtration of reaction mixture followed by the evaporation of the solvent (0.373 g, 93% yield). Big yellowish crystals of **8** (0.057 g, 14% yield) were isolated from petroleum ether at +4°C from the yellow-colored solution. This compound is only partially soluble in petroleum ether, it is completely soluble in toluene.

^{1}H NMR (tol-d$_8$, 400 MHz, 298K, δ): 0.97 (d, overlapped, $^3J_{PH}$= 14Hz, 9H, (C**H**$_3$)$_3$C), 0.97 (s, overlapped, 9H, (C**H**$_3$)$_3$C), 6.87 (m, overlapped, 4H, PPh-**H$_m$**), 6.94 (m, overlapped, 2H, PPh-**H$_p$**), 7.13 (m, overlapped, 1H, BPh-**H$_p$**), 7.29 (t, $^3J_{HH}$= 7Hz, 2H, BPh-**H$_m$**), 7.42 (broad m, overlapped, 4H, PPh-**H$_o$**), 7.51 (d, $^3J_{HH}$= 7 Hz, 2H, BPh-**H$_o$**)
^{1}H NMR (tol-d$_8$, 400 MHz, 223K, δ): 1.04 (broad m, overlapped, 18H, (C**H**$_3$)$_3$C), 6.93 (m, overlapped, 4H, PPh-**H$_m$**), 7.00 (m, overlapped, 2H, PPh-**H$_p$**), 7.16 (m, overlapped, 1H, BPh-**H$_{para}$**), 7.33 (t, $^3J_{HH}$= 8Hz, 2H, BPh-**H$_m$**), 7.51 (m, overlapped, 6H, PPh-**H$_o$** and BPh-**H$_o$**)
^{11}B NMR (tol-d$_8$, 128 MHz, δ): 80.7 (broad s, (*t*BuPhP)$_2$**B**Ph)
^{31}P{^{1}H} NMR (tol-d$_8$, 162 MHz, 298 K,δ): 42.7 (s, *t*BuPh**P**)
^{31}P{^{1}H} NMR (tol-d$_8$, 162 MHz, 223 K,δ): 41.40 (s, *t*BuPh**P**), 41.45 (s, *t*BuPh**P**)
^{13}C{^{1}H} NMR (tol-d$_8$, 100 MHz, δ): 30.9 (m, overlapped, $^3J_{CP}$= 5Hz, (**C**H$_3$)$_3$C), 34.9 (s, (CH$_3$)$_3$**C**), 126.4 (s, B**C$_p$**), 127.1 (s, B**C$_m$**), 127.4 (t, $^3J_{CP}$=5Hz, P**C$_m$**), 127.9 (s, P**C$_p$**), 128.9 (t, J= 10 Hz, B**C$_o$**), 134.5 (t, $^2J_{CP}$= 8Hz, P**C$_o$**), 135.4 (weak s, P**C$_i$**), 135.5 (weak s, P**C$_i$**), 138.8 (t, $^2J_{CP}$= 8 Hz, P**C$_o$**), 145.7 (weak broad s, B**C$_i$**)
Elemental analysis: calculated for $C_{26}H_{33}BP_2$ (M= 418.30 g/mol): %C= 74.65 %, %H= 7.95 %, found: %C= 74.17 %, %H= 7.91 %,

Synthesis of (Cy$_2$P)$_2$BPh (9)

The suspension of 0.556 g (2.72 mmol) Cy$_2$PLi in 7 mL of toluene was added dropwise to the solution of 0.337 g (1.36 mmol) PhBBr$_2$ in 3 mL of toluene. The reacting mixture was stirred in a lower temperature for another 30 min and then warmed up to room temperature and stirred for 3 days. Few colorless crystals of **9** were isolated at +4°C from the concentrated red petroleum ether solution (0.020 g, 3 % yield).

^{1}H NMR (C_6D_6, 400 MHz, δ): 1.17 (broad m, overlapped, C**H$_2$** (Cy)), 1.55 (broad m, overlapped, C**H$_2$** (Cy)), 1.65 (broad m, overlapped, C**H$_2$** (Cy)), 2.06 (broad d, J= 13 Hz, 8H, C**H$_2$** (Cy)), 2.26 (tt, J= 2 Hz, J= 12 Hz, 4H, C**H** (Cy)), 7.13 (t, $^3J_{HH}$= 7 Hz, 1H, C-**H$_{para}$**), 7.25 (t, $^3J_{HH}$= 7 Hz, 2H, C-**H$_{meta}$**), 7.50 (d, $^3J_{HH}$= 7 Hz, 2H, C-**H$_{orto}$**); It is impossible to give full integrals due to the overlapping with signals of Cy$_2$PH.
^{11}B NMR (C_6D_6, 128 MHz, δ): 71.1 (very broad s, (Cy$_2$P)$_2$**B**Ph),
^{31}P{^{1}H} NMR (C_6D_6, 162 MHz, δ): 28.0 (broad s, (Cy$_2$**P**)$_2$BNPh), -21.8 (s, Cy$_2$P-PCy$_2$), -28.1 (s, Cy$_2$PH)
^{13}C{^{1}H} NMR (C_6D_6, 100 MHz, δ): 26.0 (s, overlapped, **C**H$_2$ (Cy)), 28.2 (m, **C**H$_2$ (Cy)), 34.5 (m, overlapped, **C**H$_2$ (Cy)), 35.1 (m, **C**H (Cy), 126.7 (s, **C$_p$**), 127.1 (s, **C$_m$**), 130.3 (t, $^3J_{CP}$= 10 Hz, **C$_o$**), 146.1 (**C$_i$** - on the basis of HMBC spectrum)

Synthesis of [{(Ph$_2$P)$_2$BN*i*Pr$_2$}PtMe$_2$] (10)

The solution of 0.364 g (0.756 mmol) (Ph$_2$P)$_2$BN*i*Pr$_2$ in 2.5 mL of toluene was added dropwise to the solution of 0.252 g (0.756 mmol) CODPtMe$_2$ in 2.5 mL of toluene at -30°C. The reacting mixture was stirred in a lower temperature for another 10 min and then warmed up to room temperature. The color of the solution changed from pale yellow to dark orange and the product started to precipitate. The solvent was evaporated under reduced pressure and the residue was washed with DME and dissolved in CH_2Cl_2. Yellow crystals of **10** (0.226 g, 38 % yield) were isolated at room temperature from the orange CH_2Cl_2 solution.

^{1}H NMR ($CDCl_3$, 400 MHz, δ): 0.84 (d, $^3J_{HH}$= 7 Hz, 12 H, (C**H**$_3$)$_2$CH), 0.88 (s, $^2J_{Pt-H}$= 73 Hz, 6H, (C**H**$_3$)$_2$Pt), 3.67 (very broad s, 2H, (CH$_3$)$_2$C**H**), 5.22 (s, 2H, C**H**$_2$Cl$_2$), 7.17 (m, overlapped, 12H, C$_{Ar}$-**H**), 7.44 (m, overlapped, 8H, C$_{Ar}$-**H**)
^{11}B NMR ($CDCl_3$, 128 MHz, δ): 45.0 (broad s, (Ph$_2$P)$_2$**B**NiPr$_2$)
^{31}P{^{1}H} NMR ($CDCl_3$, 162 MHz, δ): -24.6 (broad s, $^1J_{P-Pt}$= 1406 Hz, ((Ph$_2$**P**)$_2$BNiPr$_2$)PtMe$_2$)

$^{13}C\{^1H\}$ NMR ($CDCl_3$, 100 MHz, δ): 21.9 (weak broad s, $(\mathbf{C}H_3)_2Pt$), 23.0 (s, $(\mathbf{C}H_3)_2CH$), 51.6 (broad s, $(CH_3)_2\mathbf{C}H$), 53.4 (s, $\mathbf{C}H_2Cl_2$), 128.2 (t, J_{CP}=11 Hz, $\mathbf{C_{Ar}}$), 129.3 (s, $\mathbf{C_{Ar}}$), 129.6 (weak s, $\mathbf{C_{Ar}}$), 129.8 (weak s, $\mathbf{C_{Ar}}$). 134.6 (t, J_{CP}= 10 Hz, $\mathbf{C_{Ar}}$), 136.7 (weak s, $\mathbf{C_{Ar}}$) Elemental analysis: calculated for $C_{33}H_{42}BCl_2NP_2Pt$ (M= 791.44 g/mol): %C = 50.08 %, %H= 5.35 %, %N= 1.77%, found: %C= 49.30 %, %H= 5.29 %, % N= 1.73 %;

Conflicts of interest

There are no conflicts to declare.

Acknowledgments

A.O. thank the National Science Centre, Poland (Grant 2017/25/N/ST5/00766) for financial support. R.G., N.S. and A.W. thank the National Science Centre NCN, Poland (Grant 2016/21/B/ST5/03088) for financial support. The authors thank TASK Computational Center for access to computational resources.

Notes and references

1 P. A. Chase and D. W. Stephan, *Angew. Chemie*, 2008, **120**, 7543–7547.
2 R. T. Paine and H. Nöth, *Chem. Rev.*, 1995, **95**, 343–379.
3 A. Amgoune, S. Ladeira, K. Miqueu and D. Bourissou, *J. Am. Chem. Soc.*, 2012, **134**, 6560–6563.
4 D. Dou, H. Nöth, R. T. Paine, T. Chen, E. N. Duesler and G. W. Linti, *Inorg. Chem.*, 2002, **35**, 3626–3634.
5 J. A. Bailey, M. F. Haddow and P. G. Pringle, *Chem. Commun.*, 2014, **50**, 1432–1434.
6 K. Kubo, T. Kawanaka, M. Tomioka and T. Mizuta, *Organometallics*, 2012, **31**, 2026–2034.
7 J. A. Bailey and P. G. Pringle, *Coord. Chem. Rev.*, 2015, **297–298**, 77–90.
8 H. V. R. Dias, D. C. Pestana, M. Petrie and P. P. Power, *Phosphorus. Sulfur. Silicon Relat. Elem.*, 1990, **51**, 87–91.
9 P. P. Power, *Angew. Chem. Int. Ed.*, 1990, **29**, 449–460.
10 H. Nöth, S. Staude, M. Thomann and R. T. Paine, *Chem. Ber.*, 1993, **126**, 611–618.
11 P. P. Power, A. Moezzi, D. C. Pestana, M. A. Petrie, S. C. Shoner and K. M. Waggoner, *Pure Appl. Chem.*, 1991, **63**, 859–866.
12 G. E. Coates and J. G. Livingstone, *J. Chem. Soc.*, 1961, **0**, 1000–1008.
13 H. Nöth and W. Schrägle, *Angew. Chem.*, 1962, **15**, 587.
14 G. E. Coates and J. G. Livingstone, *J. Chem. Soc.*, 1961, 5053–5055.
15 H. Nöth and S. N. Sze, *Z. Naturforsch.*, 1978, **33b**, 1313–1317.
16 G. Fritz and W. Hölderich, *Z. Anorg. Allg. Chem.*, 1977, **431**, 61–75.
17 R. A. Bartlett, H. V. Rasika Dias and P. P. Power, *Inorg. Chem.*, 1988, **27**, 3919–3922.
18 D. Dou, M. Westerhausen, G. L. Wood, G. Linti, E. N. Duesler, H. Nöth and R. T. Paine, *Chem. Ber.*, 1993, **126**, 379–397.
19 H. H. Karsch, G. Hanika, B. Huber, K. Meindl, S. König, C. Krüger and G. Müller, *J. Chem. Soc., Chem. Commun.*, 1989, 373–375.
20 M. W. Drover and J. C. Peters, *Dalton Trans.*, 2018, **47**, 3733–3738.
21 A. Lik, D. Kargin, S. Isenberg, Z. Kelemen, R. Pietschnig and H. Helten, *Chem. Commun.*, 2018, **54**, 2471–2474.
22 K. Kaniewska, A. Dragulescu-Andrasi, Ł. Ponikiewski, J. Pikies, S. A. Stoian and R. Grubba, *Eur. J. Inorg. Chem.*, 2018, 4298–4308.
23 N. Szynkiewicz, Ł. Ponikiewski and R. Grubba, *Dalton Trans.*, 2018, **47**, 16885–16894.
24 P. Pyykkö and M. Atsumi, *Chem. - A Eur. J.*, 2009, **15**, 186–197.
25 P. Pyykkö and M. Atsumi, *Chem. - A Eur. J.*, 2009, **15**, 12770–12779.
26 D. C. Pestana and P. P. Power, *Organometallics*, 1992, **11**, 98–103.
27 H. Beall and C. H. Bushweller, *Chem. Rev.*, 1973, **73**, 465–486.
28 D. Imbery, A. Jaeschke and H. Friebolin, *Org. Magn. Reson.*, 1970, **2**, 271–281.
29 C. Brown, R. H. Cragg, T. J. Miller and D. O. Smith, *J. Organomet. Chem.*, 1983, **244**, 209–215.
30 D. C. Pestana and P. P. Power, *J. Am. Chem. Soc.*, 1991, **113**, 8426–8437.
31 T. Tanaka and N. Watanabe, *Org. Magn. Reson.*, 1974, **6**, 165–169.
32 U. Berg and J. Sandström, in *Advances in Physical Organic Chemistry*, 1989, vol. 25, pp. 1–97.
33 A. Lik, L. Fritze, L. Müller and H. Helten, *J. Am. Chem. Soc.*, 2017, **139**, 5692–5695.
34 A. Shvartsbart and A. B. Smith, III, *J. Am. Chem. Soc.*, 2014, **136**, 870–873.
35 J. X. Mcdermott, J. F. White and G. M. Whitesides, *J. Am. Chem. Soc.*, 1976, **98**, 6521–6528.
36 E. Costa, P. G. Pringle and M. Ravetz, *Inorg. Synth.*, 1997, **31**, 284–286.